Author/s:
Habiba, U;Merlin, S;Lim, JKH;Wong, VHY;Nguyen, CTO;Morley, JW;Bui, BV;Tayebi, M

Title:
Age-Specific Retinal and Cerebral Immunodetection of Amyloid-β Plaques and Oligomers in a Rodent Model of Alzheimer's Disease

Date:
2020-01-01

Citation:
Habiba, U., Merlin, S., Lim, J. K. H., Wong, V. H. Y., Nguyen, C. T. O., Morley, J. W., Bui, B. V. & Tayebi, M. (2020). Age-Specific Retinal and Cerebral Immunodetection of Amyloid-β Plaques and Oligomers in a Rodent Model of Alzheimer's Disease. Journal of Alzheimer S Disease, 76 (3), pp.1135-1150. https://doi.org/10.3233/JAD-191346.

Journal of Alzheimer's Disease xx (20xx) x–xx
DOI 10.3233/JAD-191346
IOS Press

Age-Specific Retinal and Cerebral Immunodetection of Amyloid-β Plaques and Oligomers in a Rodent Model of Alzheimer's Disease

Umma Habiba[a], Sam Merlin[b], Jeremiah K.H. Lim[c], Vickie H.Y. Wong[c], Christine T.O. Nguyen[c], John W. Morley[a], Bang V. Bui[c] and Mourad Tayebi[a,*]
[a]*School of Medicine, Western Sydney University, Campbelltown, NSW, Australia*
[b]*School of Science & Health, Western Sydney University, Campbelltown, NSW, Australia*
[c]*Department of Optometry and Vision Sciences, University of Melbourne, Victoria, Australia*

Accepted 18 May 2020

Abstract.
Background: Amyloid-β soluble oligomers (Aβo) are believed to be the cause of the pathophysiology underlying Alzheimer's disease (AD) and are normally detected some two decades before clinical onset of the disease. Retinal pathology associated with AD pathogenesis has previously been reported, including ganglion cell loss, accumulation of Aβ deposits in the retina, and reduction of nerve fiber layer thickness as well as abnormalities of the microvasculature.
Objective: This study's aim is to better understand the relationship between brain and retinal Aβo deposition and in particular to quantify levels of the toxic Aβo as a function of age in the retina of a rodent model of AD.
Methods: Retinas and brain tissue from 5×FAD mice were stained with Congo red, Thioflavin-T (Th-T), and Aβ plaque-specific and Aβo-specific antibodies.
Results: We show that retinas displayed an age-dependent increase of Th-T-specific amyloid fibrils. Staining with anti-Aβ antibody confirmed the presence of the Aβ plaques in all 5×FAD retinas tested. In contrast, staining with anti-Aβo antibody showed an age-dependent decrease of retinal Aβo. Of note, Aβo was observed mainly in the retinal nuclear layers. Finally, we confirmed the localization of Aβo to neurons, typically accumulating in late endosomes, indicating possible impairment of the endocytic pathway.
Conclusion: Our results demonstrate the presence of intraneuronal Aβo in the retina and its accumulation inversely correlated with retinal Aβ plaque deposition, indicating an age-related conversion in this animal model. These results support the development of an early AD diagnostic test targeting Aβo in the eye.

Keywords: Anti-oligomer antibody, Alzheimer's disease, amyloid-β oligomers, retina, retinal immunodetection, 5×FAD mice

INTRODUCTION

Alzheimer's disease (AD) is a progressive neurodegenerative disorder associated with a gradual decline in cognitive function, memory loss, abnormal behavior, and reduction of brain volume [1–4]. The neuropathological lesions observed in the brain

*Correspondence to: Dr. Mourad Tayebi, Associate Professor in Biomedical Sciences, School of Medicine, Western Sydney University, Campbelltown, NSW, Australia. Tel.: +61 (02) 4620 3671; E-mail: m.tayebi@westernsydney.edu.au.

of AD patients include extracellular deposition of amyloid-β (Aβ) plaques; intracellular deposition of hyperphosphorylated tau protein in the form of neurofibrillary tangles, ubiquitin, cerebral amyloid angiopathy, severe synaptic loss, and neuronal death [2, 3, 5, 6]. Brain accumulation of misfolded/aggregated Aβ is believed to be one of the major pathological constituents for the development of the disease. Aβ peptide is derived from a larger protein, namely the amyloid-β protein precursor (AβPP) [5]. AβPP is enzymatically cleaved into amyloidogenic and non-amyloidogenic entities. In AD, the β- and γ-secretase sequentially cleave AβPP and produce the Aβ peptide fragments (36–43 amino acids) [7–9], that aggregate and lead to accumulation of brain deposits or plaques [6, 10, 11]. Enzymatic cleavage leads to the formation of two major isoforms of Aβ; $A\beta_{40}$ (∼80–90%) and $A\beta_{42}$ (∼5–10%) [5, 12, 13]. In sporadic and familial AD, three major assemblies of Aβ have been reported [11, 14, 15], including monomeric Aβ composed of low molecular weight dimers and trimers; soluble oligomers, containing 12–24 monomers which become elongated to form protofibrils; and insoluble fibrils [16, 17]. Aβ soluble oligomers (Aβo) are neurotoxic and responsible for triggering the pathophysiology of AD [18–21]. Experimental detection of Aβo in peripheraltissues and/or blood precedes its central accumulation in the brain by some two decades [22, 23], highlighting Aβo as a potential early diagnostic marker.

Various diagnostic approaches have been used for the detection of AD, which include neuroclinical and neuropsychological examinations, blood and cerebrospinal fluid (CSF) screening, and brain imaging. However, most of these approaches are non-specific, and some are invasive, expensive, and time-consuming. Thus, there is an urgent need for a non-invasive and cost-effective diagnostic screen to identify AD-affected subjects in the preclinical or early clinical stages. Visual disturbances are often an early complaint reported by AD patients [24, 25], and have been linked to abnormalities of ocular physiology [26–32]. Patients experience altered color vision [33, 34], peripheral vision loss [35–37], and modified sensitivity to contrast and sometimes visual acuity [33, 38]. Alteration of retinal morphology has been reported in AD patients and include changes to the vasculature [26], optic nerve head [39], ganglion cell and axon loss [40, 41], and thinning of the retinal nerve fiber layer [28, 40–50]. A study by O'Bryhim and colleagues using optical coherence tomography and angiography demonstrated that individuals with preclinical AD displayed early retinal architecture and vascular changes [51]. Another study demonstrated the feasibility to noninvasively detect and quantify, using a clinical scanning laser ophthalmoscope, amyloid deposits in the retina of human subjects given an oral solid lipid curcumin fluorochrome [47]. Koronyo et al. show in some cases that Aβ deposits in the retina was associated with blood vessels similar to cerebral vascular amyloid pathology [47] supporting other studies which indicate alteration to retinal vasculature [52–54]. While Aβ deposits have been reported in the retina, how such levels change with age is not well documented. Furthermore, the relationship between retinal and brain soluble Aβo and insoluble oligomers is not well understood.

In this report, we assess in the 5×FAD mouse model age-related Aβo and Aβ plaque burden in the retina and brain of 6- to 17-month-old animals. Oakley and colleagues developed the 5×FAD, a transgenic rodent model that co-expresses five mutations [AβPP K670N/M671L (Swedish) + I716V (Florida) + V717I (London) and PS1 M146L+L286V] that displays intraneuronal accumulation of $A\beta_{42}$ before plaque formation [55]. We show that retinal accumulation of Aβo was similar to brain in the early stage of the disease and their levels were inversely proportional to the age-related increased in Aβ plaque increase.

We showed that Aβo was colocalized to late-endosomal compartments in retinal neurons, indicating impairment in their ability to process and degrade this oligomeric species. Our study highlights the possibility of targeting Aβo in the eye apreclinical diagnostic test for AD.

MATERIALS AND METHODS

Animals

The 5×FAD transgenic mice were made by co-injecting two vectors encoding AβPP (with Swedish (K670N/M671L), Florida (I716V), and London (V717I) mutations and PSEN1 (with M146L and L286V mutations), each driven by the mouse Thy1 promoter. This strain does not carry the retinal degeneration allele *Pde6b*^{rd1}. The 5×FAD mouse model rapidly develops severe amyloid pathology. Plaques spread throughout the hippocampus and cortex by six months of age. Synapse degeneration, neuronal loss and deficits in spatial learning are observed at approximately four months [55]. Age-matched wild

type littermates were used as controls (Supplementary Table 1).

All procedures followed the requirements of the National Health and Medical Research Council of Australia statement for the use of animals in research, the Association for Research in Vision and Ophthalmology (ARVO) Statement for the Use of Animals in Ophthalmic and Vision, and were approved by the Howard Florey Animal Ethics Committee (13-068-UM). Mice were housed with free access to water and normal rodent chow (Barastoc, Melbourne, VIC, Australia) in the Melbourne Brain Centre (Parkville, VIC, Australia). Room temperature was maintained at 21°C, with animals exposed to a 12 h light/dark cycle (on at 7 AM, <50 lux inside the cage).

Tissue collection and histological assessment of brains and eyes

All mice (Supplementary Table 1) were perfused with saline and 10% neutral buffered formalin. Mouse brains and eyes were then fixed in 10% neutral buffered formalin, dehydrated using graded ethanol, washed with xylene, and finally embedded in paraffin. $3 \times 6\,\mu$m sections of each brain and retinal tissue were cut with a microtome (Thermofisher Scientific, Waltham, MA, USA) and then processed for routine hematoxylin and eosin (H & E), Congo red, and Thioflavin T (ThT) staining as well as immunohistochemistry and immunofluorescence. Sections were deparaffinized with xylene and rehydrated through graded alcohols and finally deionized water.

Congo red Aβ staining

Sections were placed in Congo red (Leica biosystems, Wetzlar, Germany) working solution for 20 min then rinsed in 5–8 changes of deionized water. This was followed by staining in Gill llHematoxylin (Leica biosystems) for 1–3 min and rinsing in three changes of deionized water. Sections were dehydrated in two changes of 95% alcohol and three changes of absolute alcohol for 1 min each. Finally, sections were cleared in two changes of xylene and mounted in a xylene miscible medium. Amyloid fibrils appeared as dull to brick red under light microscopy (Olympus CX 43, Shinjuku, Tokyo, Japan) and apple green birefringence under polarized light (Olympus CX 43).

Thioflavin-T staining of Aβ plaques

Following deparaffinization with xylene and ethanol, tissue sections were incubated in filtered 1% aqueous ThT (Sigma-Aldrich, St. Louis, MO, USA) for 8 min at room temperature. Sections were then rinsed in three changes of deionized water and mounted in aqueous mounting media (Agilent, Santa Clara, CA, USA). Finally, slides were sealed with clear nail polish and stored in a cold and dark place. Generally, ThT binds to the side chain channels along the long axis of amyloid fibrils. Upon binding to amyloid fibrils, ThT has a strong signal at excitation and emission maxima of 450 and 482 nm, respectively under fluorescence microscopy (Olympus VS 120).

Immunohistochemical assessment of Aβ plaques and soluble oligomers

Sections were pre-treated with antigen retrieval method (1× citrate buffer for 20 min in a water bath; pH 6) to expose the target antigen. Sections were then treated with 90% formic acid for 5 min at room temperature followed with cell membrane permeabilization which was achieved using 1% triton X for 1 min prior to addition of 0.3% H_2O_2 for 15 min to inactivate endogenous peroxidases. Sections were then blocked with Protein Block Serum-Free (Agilent, Santa Clara, CA, USA) for 15 min. Sections were then stained for 1 h with the following primary antibodies in PBS: mouse purified *4G8* anti-Aβ against 17–24 of Aβ peptide (1 : 500; Bio legend, San Diego, CA, USA) or *A11* rabbit anti-Aβo Antibody (1 : 250; Merck Millipore, Burlington, MA, USA) respectively. Sections were also stained with IgG1 isotype control (BRIC 222 recognizing CD44 [56] or IgG2b isotype control (BRIC 126 recognizing CD47 [57] antibodies to confirm specificity and selectivity of both A11 and 4G8 antibodies. Next, sections were incubated for 1 h at room temperature with secondary antibodies in PBS: HRP-conjugated anti-mouse IgG(Sigma-Aldrich) or anti-rabbit IgG (Sigma-Aldrich) respectively. After washing three times with PBS, sections were covered with DAB solution and incubated for 5–10 min. Slides were then counterstained with hematoxylin for 1 min then imaged using the Olympus VS 120 Slide Scanner and were analyzed using 'Olympus OlyVIA' software.

Immunofluorescence co-localization studies

Double immuno-labelling was achieved by two different fluorescent labels, each having a separate emission wavelength. Sections were incubated overnight with both *A11* and *4G8* at 4°C. Further, and in other experiments, sections were incubated

with *A11* and mouse Anti-*NeuN* mAb, clone A60 (Merck Millipore) to demonstrate neuronal homing of the oligomers. Additionally, sections were incubated with *A11* and mouse anti-lysosomal-associated membrane protein 2 (*LAMP2*, Stressgen Bio reagents Corp, Victoria, British Columbia, Canada) antibodyto assess whether Aβo localize to lysosomes/late endosomes. In both cases sections were incubated overnight at 4°C. Sections were then incubated with goat anti-rabbit IgG conjugated to FITC (Sigma-Aldrich) and donkey anti-mouse IgG conjugated to Texas red (Sigma-Aldrich) respectively for 2 h at 4°C. Sections were then mounted using fluorescence mounting media (Agilent, Santa Clara, CA, USA). Finally, the mounted sections were imaged using Olympus VS 120 Slide Scanner with a standard FITC/Texas Red double band-pass filter set.

Image quantification

Three sections from different 5×FAD and wild type mice were used for image quantification (Supplementary Figure 1). Three different areas of hippocampus, cerebral corte, × and retina were analyzed. Immunofluorescence signal intensity was visualized by capturing red and green fluorescent field images using the Olympus VS 120 Slide Scanner. Images were analyzedusing 'Olympus OlyVIA' software. Age-dependent accumulation of Aβ plaques and Aβo in 5×FAD was quantified using image processing software, *cellSense* (Olympus). The mean color threshold of fluorescent particles (red particles for plaques and green particles for oligomers) was calculated in several brain regions and eyes for each age group and the final result was presented as percentage fluorescence intensity and expressed as mean ± S.E.M.

Statistical analysis

One-way ANOVA with Dunnett's post-test was performed using GraphPad Prism version 7.00 for Windows (GraphPad, San Diego, CA, USA), for statistical analysis.

RESULTS

Histological assessment of retinal and cerebral lesions in 5×FAD mice

We first performed an initial assessment to confirm the presence of the typical neuropathological lesions associated with AD in the brain and retina of the 6–7-month-old 5×FAD mice (Fig. 1). H & E stain displayed widespread vacuolations, neuronal death, and presence of eosinophilic structures in the cortical and hippocampal region of the brain (Fig. 1C), in contrast with the retina which at the same age did not display the above structural changes (Fig. 1D).

Retinal and cerebral detection of Congophilic and ThT-specific Aβ fibrils in 5×FAD mice

One of the distinctive neuropathological features associated with human AD brains is the presence of extracellular Aβ plaques [4, 6, 58]. We initially used Congo red and ThT [59] to assess age-dependent accumulation of amyloid fibrils and compare amyloid burden in the retinas and brains derived from 6-, 7-, 12-, 14-, and 17-month-old 5×FAD and WT mice (Fig. 2). Here, we show the distinctive Congophilic red-brick coloration confirming the presence of amyloid fibrils in the brain and retina starting from 6 months (Fig. 2A, B) of age, respectively. This was confirmed by the presence of apple-green birefringence when examined under cross-polarized light (Fig. 2C, D). However, retinal apple-green birefringence was less intense compared to the brain. This pattern of amyloid fibrils distribution in retina and brain in these different age groups was confirmed with ThT staining; which displayed more pronounced staining in all age groups tested starting from 6 months onward (Fig. 2E, F). Congophilic- and ThT-specific retinal amyloid fibrils were clearly visible in the inner nuclear layer (INL), inner plexiform layer (IPL), and the ganglion cell layer (GCL) of all age groups (Fig. 2F). These results confirm that the retina of the 5×FAD mice show signs of AD pathogenesis [37]. Of note, Congophilic- and ThT-specific amyloid fibrils were not visible in the brains and retinas of the age-matched 6-month-oldwild type littermates (Supplementary Figure 2).

Retinal and cerebral immunodetection of Aβ plaques and Aβsoluble oligomers in 5×FAD mice

5×FAD mice are known to exhibit cerebral accumulation of intracellular Aβo and extracellular Aβ plaques [55]. Although, amyloid fibrils are a neuropathological hallmark of human AD, there is strong evidence that oligomers are the most toxic species and appear to be the main causative agent of neurological deficits [20, 60]. Moreover, it is now recognized

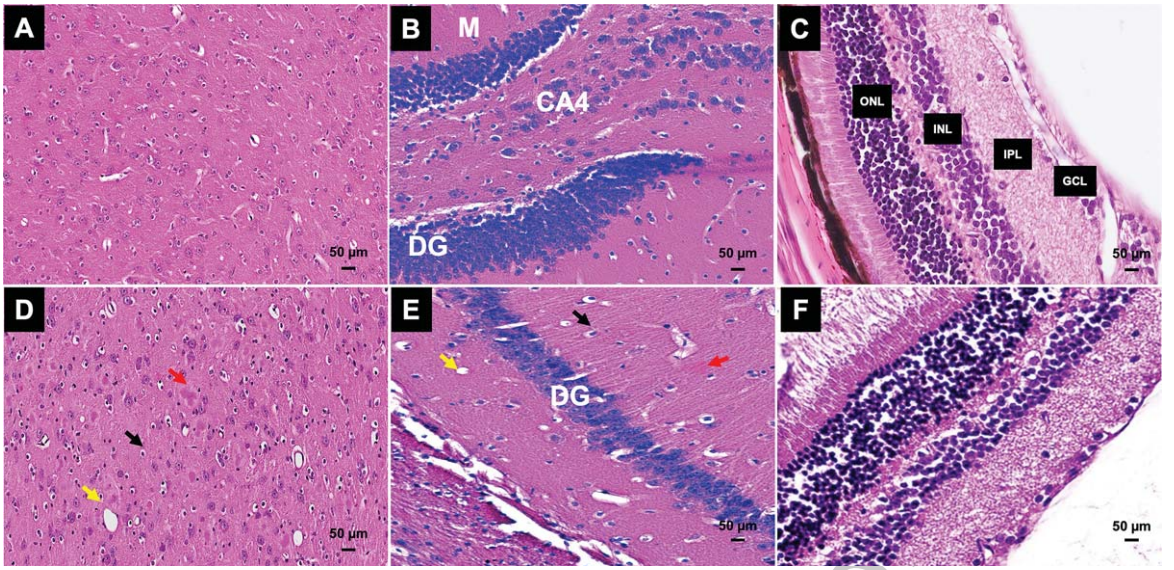

Fig. 1. Photomicrographs of the microscopic lesions in the brains and retinas of six-month-old 5×FAD mice. A) Normal appearance of the cerebral cortex in a healthy wild type mouse following staining with H & E. B) Normal appearance of the hippocampus in a healthy wild type mouse following staining with H & E (M, molecular layer; CA4, Cornu Ammonis 4; DG, dentate gyrus). C) Normal appearance of the retina in a healthy wild type mouse following staining with H & E. The photomicrograph was derived from peripheral region of the retina, away from the optic disc. Widespread vacuolations, neuronal death, and presence of eosinophilic structures in a 6-month-old 5×FAD mouse brain. Vacuolations (yellow arrow), neuronal death (black arrow), and eosinophilic structures (red arrows) are observed in the D) cortical and E) hippocampal region of the brain following staining with H & E (DG, dentate gyrus). F) Normal appearance of the retina in a 6-month-old 5×FAD mouse brain following staining with H & E. The photomicrograph was derived from peripheral region of the retina, away from the optic disc. Representative of all affected mice in this age group.

that Aβo accumulation inserum of AD patients and experimental models can occur years before plaque build-up in the brain [61–63]. We hypothesized that Aβo accumulation in the retina might also precede cerebral plaque build-up in 5×FAD mice in an age-dependent manner. We initially examined brains and retinas for the presence of Aβo and Aβ plaques by immunohistochemistry using *A11* and *4G8,* respectively (Figs. 3–5). 6-month-old 5×FAD mice displayed abundant intraneuronal Aβo deposits in the cerebral cortex, hippocampus, retinal nuclear layers (INL & ONL), and GCL (Fig. 3A–C) as well as few extracellular Aβ plaques (Fig. 3D–F). Interestingly, 12-month-old 5×FAD mice exhibited more pronounced extracellular cortical and hippocampal Aβ plaques but lower levels of intracellular Aβo compared to the 6-month-old age group (Fig. 4A–F). Nonetheless, levels of intracellular Aβo appeared lower in these brain structures compared to the 6-month-old age group (Fig. 4A, B). Similarly, retinal Aβo which could be seen in the GCL, INL, and ONL appeared less abundant in this age group compared to the 6-month-old mice (Fig. 4C). Occasional Aβ plaques were also evident in the retinal layers of 12-month-old 5×FAD mice, and their levels appeared lower than the 6-month-oldage group (Fig. 4F). As the age of the 5×FAD mice progressed, fewer intracellular Aβo deposits were observed as opposed to the abundant accumulation of Aβ plaques in the cerebrum of 14- and 17-month-old mice (Fig. 5). Retinal Aβ plaques were also conspicuous in the ganglion layer but Aβo appeared to be absent in the 14- and 17-month-old 5×FAD mice (Fig. 5C, F). No Aβo and Aβ plaques deposits were seen in age-matched wild type littermates (data not shown). These results support previous findings that Aβ plaque burden increased over the course of the disease in both brain and retina, whereas Aβo levels appear to decrease in an age-dependent manner [64].

Aβ oligomers co-accumulate with Aβ plaques and co-localize with an endosomal marker in neurons of 5×FAD mice

Our immunostaining results confirmed that accumulation of intracellular Aβo and Aβ plaques in the retinal layers parallels their brain build-up. We then investigated whether Aβo and Aβ plaques co-localize/accumulate in different regions and structures of the retina and brain of the various age groups

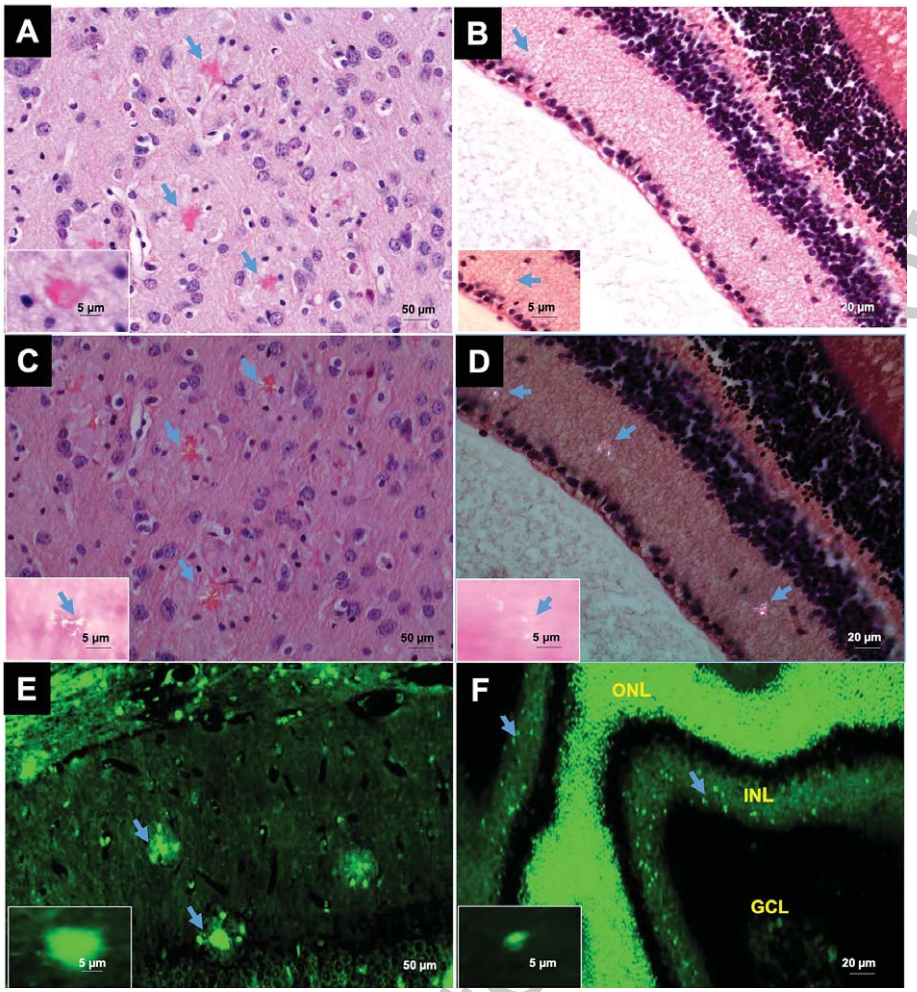

Fig. 2. Photomicrographs of Congo red- and Thioflavin T-specific amyloid-β fibrils in the brains and retinas of six-month-old 5×FAD mice. A) Distinctive red-brick staining of amyloid fibrils with Congo red in the brain and B) GCL and ONL of the retina of a 6-month-old 5×FAD mouse. The photomicrograph was derived from peripheral region of the retina, away from the optic disc. The presence of the amyloid fibrils was confirmed with the presence of apple-green birefringence in the C) brain and D) retina under polarized light. Thioflavin T staining displayed presence of amyloid fibrils in the E) hippocampus and in the F) INL, IPL, and GCL of the retina (blue arrows). Representative of all affected mice in this age group.

tested using *A11* and *4G8* (Supplementary Figure 3). This immunofluorescence study confirmed the presence of intracellular Aβo and Aβ plaques in the retina of the 6-month-old 5×FAD mice (Supplementary Figure 3). Here, retinal Aβo was more prominent in the GCL and INL, and to a lesser extent in the IPL and ONL (Supplementary Figure 3). While present, retinal Aβ plaques were less prominent in this age group (Supplementary Figure 3). Remarkably, both Aβo and Aβ plaques were widespread in hippocampus and cerebral cortex of the 6-month-old 5×FAD mice (Supplementary Figure 4). At 12months of age, retinal oligomers and plaques co-localized in the GCL, INL, IPL, and ONL (Supplementary Figure 3) and co-accumulated and displayed very strong staining in the cerebral cortical region and hippocampus (Supplementary Figure 4). The immunofluorescence studies appeared to be more sensitive than immunohistochemistry as the latter allowed stronger detection of retinal Aβ plaques in the 12-month-old 5×FAD mice. Surprisingly, Aβo were detected in the retina and cerebrum of the 17-month-old 5×FAD mice (Supplementary Figures 3 and 4). Finally, and as expected, the 17-month-old 5×FAD mice displayed conspicuous widespread accumulation of cerebral Aβ plaques, which were also observed in the retinas of these animals (Supplementary Figures 3 and 4). No staining for both Aβo and Aβ plaques was

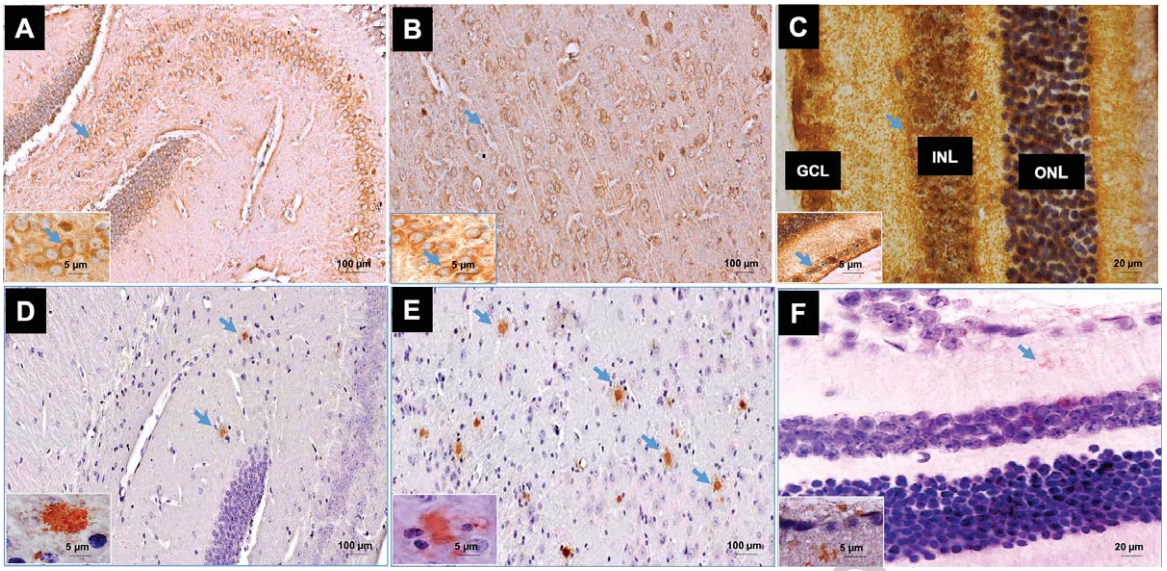

Fig. 3. Photomicrographs of the amyloid-β oligomers and plaques in the brain and retina of a six-month-old 5×FAD mouse. A) Immunohistochemical staining with A11 rabbit anti-Aβo polyclonal IgG antibody of a 6-month-old 5×FAD mouse which shows intraneuronal stained structures in the A) hippocampus, in the B) cerebral cortex and in the C) GCL, INL, and ONL of the retina. The photomicrograph was derived from peripheral region of the retina, away from the optic disc. D) Immunohistochemical staining with 4G8 murine anti-Aβ monoclonal IgG antibody of a 66-month-old5×FAD mouse which shows characteristic extracellular AD Aβ plaques in the D) hippocampus, in the E) cerebral cortex and in the F) GCL and ONL of the retina. CA4, DG, and M refers to hippocampal Cornu Ammonis, Dentate gyrus, and the molecular layer, respectively. Representative of all affected mice in this age group.

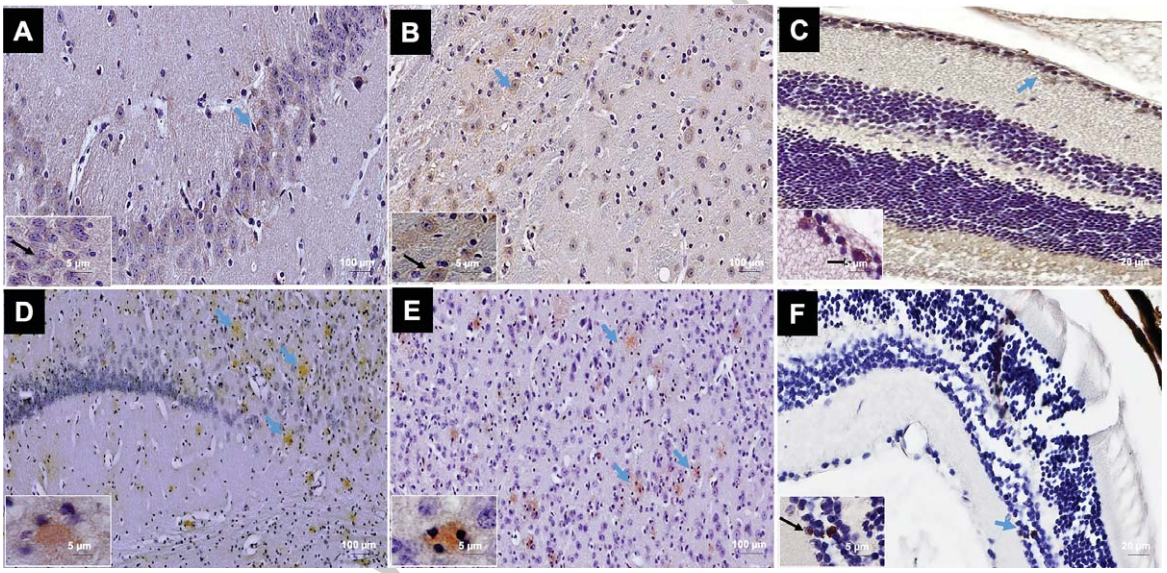

Fig. 4. Photomicrographs of the amyloid-β oligomers and plaques in the brain and retina of a twelve-month-old 5×FAD mouse. A) Immunohistochemical staining with A11 rabbit anti-Aβo polyclonal IgG antibody of a 12-month-old 5×FAD mouse which shows less intense intraneuronal stained structures in the A) hippocampus, in the B) cerebral cortex and in the C) GCL of the retina (arrows). The photomicrograph was derived from peripheral region of the retina, away from the optic disc. Immunohistochemical staining with 4G8 murine anti-Aβ monoclonal IgG antibody of a 12-month-old 5×FAD mouse which shows widespread and intense staining of the extracellular AD Aβ plaques in the D) hippocampus, and in the E) cerebral cortex (arrows). E) Very few plaques were observed in the retina (arrows). CA3, DG, and M refers to hippocampal Cornu Ammonis, Dentate gyrus, and the molecular layer, respectively. Representative of all affected mice in this age group.

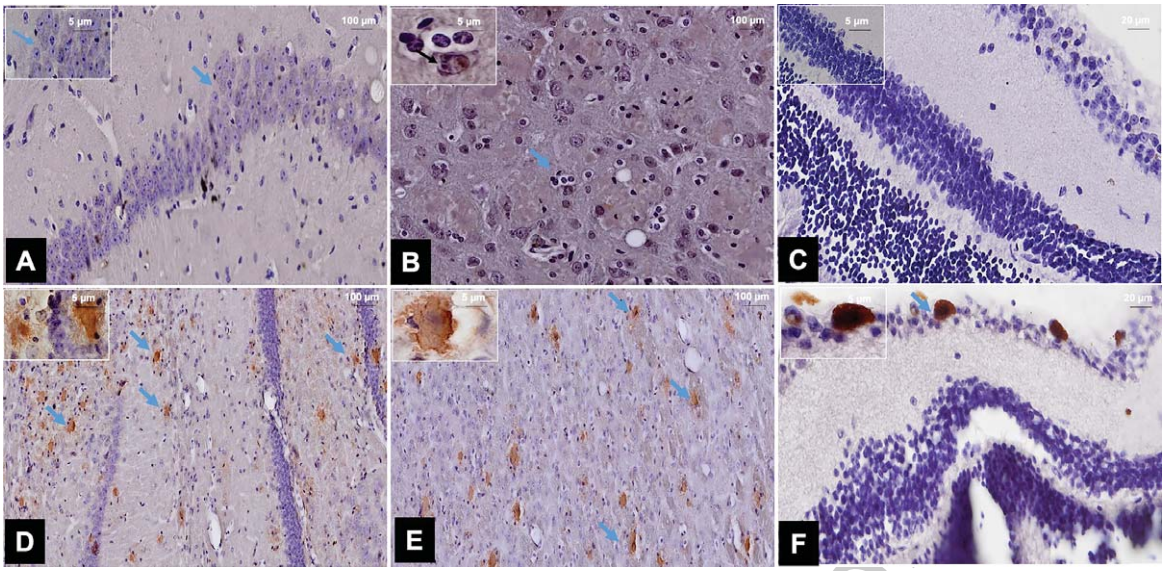

Fig. 5. Photomicrographs of the amyloid-β oligomers and plaques in the brain and retina of a seventeen-month-old 5×FAD mouse. A) Immunohistochemical staining with A11 rabbit anti-Aβo polyclonal IgG antibody of a 17-month-old 5×FAD mouse which shows scarce intraneuronal stained structures in the hippocampus, and in the B) cerebral cortex (arrows). C) Aβo were absent in the retina in this age group. The photomicrograph was derived from peripheral region of the retina, away from the optic disc. D) Immunohistochemical staining with 4G8 murine anti-Aβ monoclonal IgG antibody of a 17-month-old 5×FAD mouse which shows widespread and intense staining of the extracellular AD Aβ plaques in the hippocampus, and in the E) cerebral cortex (arrows). F) Plaques were observed in the GCL of the retina (arrows). CA1, DG, and M refers to hippocampal Cornu Ammonis, Dentate gyrus, and the molecular layer, respectively. Representative of all affected mice in this age group.

seen in all brain and retinas of wild type age group (data not shown).

Immunofluorescence signal intensity of both Aβ plaques and oligomers were quantified by an image processing software, *cellSense* (Fig. 6) in the retina, hippocampus, and cortex of the 6-month ($n=5$), 12-month ($n=5$), and ≥14-month ($n=7$) 5×FAD groups and compared with 6–7-month ($n=5$), 12-month ($n=6$), and 14-month ($n=5$) wild type littermates. Of note, three different areas of each section were analyzed. Aβ plaque loads significantly increased from 6 months and onward ($p<0.001$) in the retina (Fig.6G, I), hippocampus (Fig. 6D, F), and cortex (Fig. 6A, C) of the 6–7-, 12-, and ≥14-month-old age 5×FAD groups. In contrast, Aβ oligomers levels significantly decreased between 6-7 months and 12 months ($p<0.001$) in the retina (Fig. 6H, I), hippocampus (Fig. 6E, F), and cortex (Fig. 6B, C) of the 6–7-month, 12-month, and ≥14-month-old age 5×FAD groups.

Disturbances of the endosomal/lysosomal system is thought to be involved in neuronal toxicity and Aβ accumulation [65]. Inhibition of Aβ secretion can lead to intraneuronal Aβ accumulation in the endosomal/lysosomal compartment, which destabilizes its membrane leading to Aβ deposition in the cytosolic compartment [66–68]. To verify the presence of Aβo deposits in the brain and retinal endosomal/lysosomal, we co-stained *A11* and *LAMP2*, a marker against late endosome and lysosomes (Fig.7). Our data showed that Aβo co-localized with the lysosomal marker in the hippocampus, cortex and in the ONL, OPL, and INL of the retina in all age groups (Fig. 7A–F). Our results strongly indicate binding of *A11* antibody in these organelles where clearance of Aβo is believed to occur. Finally, we confirmed that Aβo accumulation was in fact occurring in cerebral and retinal neurons as evident by co-staining with *NeuN* in all age groups (Fig. 7G, H). Moreover, Aβo deposits were more prominent in the retinal GCL and INL in the retina in the 6-month-old age group (Fig. 7H).

DISCUSSION

One of the principal neuropathological lesions associated with AD is the extracellular deposition of Aβ plaques [6]. Among the three major assemblies of Aβ, soluble oligomers are considered the most neurotoxic form and is the intermediary conforma-

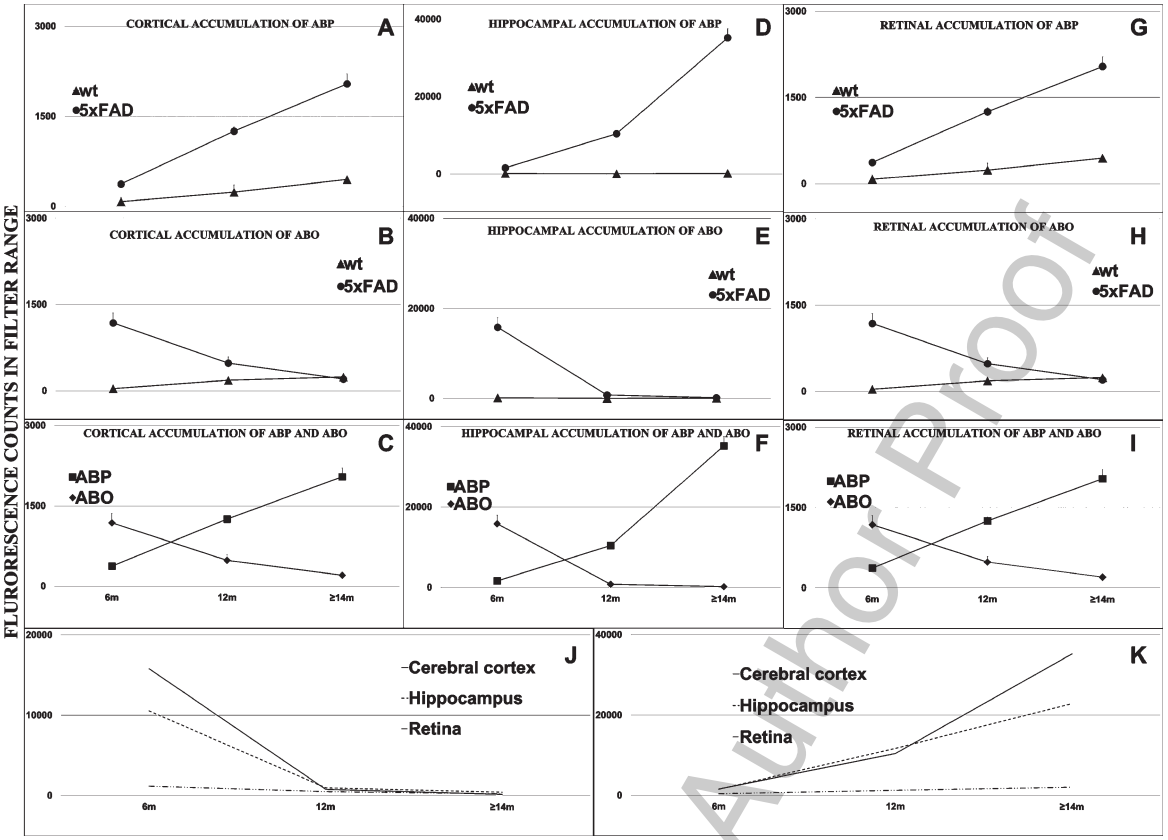

Fig. 6. Quantification of amyloid-β plaque burden and amyloid-β oligomers with CellSense image processing software. Total Aβ plaque burden (ABP) in the cerebral cortex (A, C, J), hippocampus (D, F, J), and retina (G, I, J) was quantified in 6–7-month-old (5×FAD = 5; wild type = 5); 12-month-old (5×FAD = 6; wild type = 6); and ≥14-month-old (5×FAD = 7; wild type = 5). Total Aβ oligomer load (Aβo) in the cerebral cortex (B, C, K), hippocampus (E, F, K), and retina (H, I, K) was quantified in 6-month-old (5×FAD = 5; wild type = 5); 12-month-old (5×FAD = 6; wild type = 6); and ≥14-month-old (5×FAD = 7; wild type = 5). Data represents mean ± SEM.

tion recognized in early pathogenesis [11]. Soluble oligomers can lead to synaptic dysfunction, whereas large, insoluble deposits are believed to function as reservoirs of the bioactive oligomers [19]. In AD, Aβo are believed to form in the early phase of the disease and are present in blood and other tissues [69–71]. Current strategies for AD detection include measurement of CSF-borne $A\beta_{42}$ levels and amyloid positron emission tomography (PET) imaging [70]. However, these approaches are considered to be invasive, display a high degree of multicenter variability, and are costly. A blood-based biomarker approach is gaining momentum as several groups have demonstrated its potential value, albeit work remains at experimental phase [72, 73]. Since Aβo is considered the toxic species and accumulates in preclinical stage of the disease [74–77], several reports have demonstrated its potential as an early marker of the disease [78–80]. A recent study by Nakamura and colleagues has identified high-performance plasma Aβ biomarkers using a combination of immunoprecipitation and mass spectrometry [81]. These authors measured and compared $A\beta PP_{669-711}/A\beta_{1-41}$ and $A\beta_{1-40}/A\beta_{1-41}$ ratios in order to predict Aβ-PET imaging status in cognitively normal, mild cognitive impaired, and AD individuals and shown that this test was highly predictive of brain Aβ burden.

In this study, we set out to provide proof-of-concept for early retinal detection of AD through identifying and quantifying levels of retinal Aβo in an AD mouse model. The eye is not considered as a hermetic anatomical structure and the barriers that separate the eye from the periphery are not completely sealed [82]. The blood-ocular barriers comprise the blood-retinal and blood-aqueous barrier; the latter is formed by tight junctions of the inner non-pigmented ciliary epithelium and the non-fenestrated endothelial cells of the iris blood vessels [82]. In contrast and because

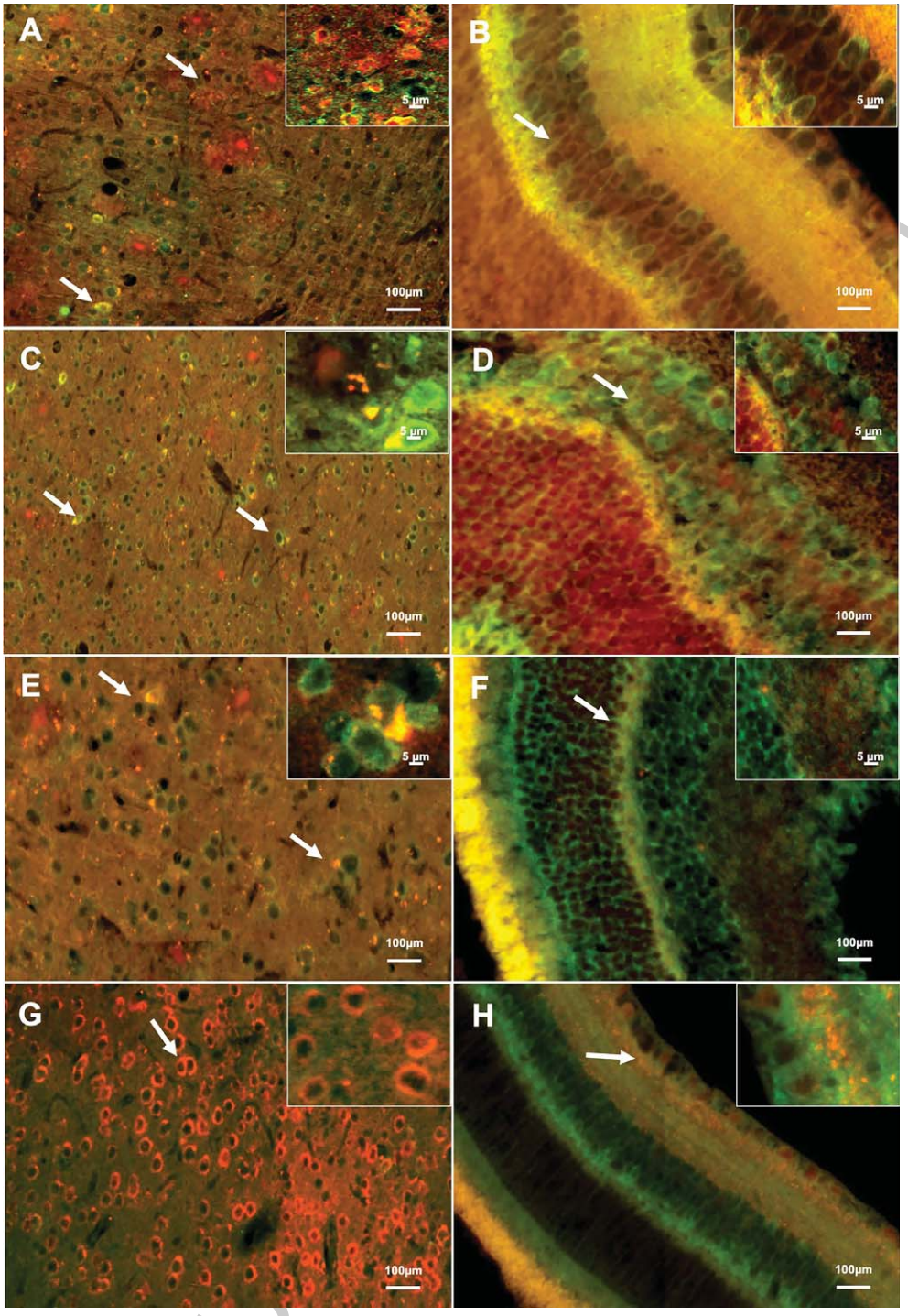

Fig. 7. Immunofluorescence co-localization of retinal and cerebral amyloid-β oligomers with lysosomal-associated membrane protein 2 (LAMP2) or neuron-specific nuclear protein (NeuN). Retinal and cerebralco-staining with A11 rabbit anti-Aβo polyclonal IgG antibody (green) and anti-mouse LAMP2 monoclonal IgG antibody (red) of a 6-, 12-, and 17-month-old 5×FAD mice or anti-mouse NeuN monoclonal IgG antibody (red) of a 6-month-old 5×FAD mouse. LAMP2 co-localized with Aβo in the (A, C, E) cerebral cortex and (B, D, F) in the GCL, IPL, INL, OPL, and ONL of the retina in all age groups (arrows). Aβo localized to NeuN in the (G) hippocampus, and in the (H) GCL, IPL, INL, and OPL of the retina in the 6-month-old age group (arrows). Representative of all affected mice in all age groups.

of the fenestrated structure of the ciliary body blood vessels, plasma proteins and molecules can enter the stroma as part of aqueous humor production [82]. Therefore, there is a distinct possibility that blood borne-Aβo might reach different structures of the eye, including the retina, and this provides a great potential to develop a non-invasive retinal eye test for AD. Of note, eye inflammation leads to blood-ocular barrier disruption, which also results in increased vascular permeability, potentially allowing higher levels of Aβo to spread in all structures of the eye.

Visual disturbances are part of early complaints reported by AD patients [83]. These disturbances include reduced blood vessel diameter and venous blood flow. Studies by Berisha and colleagues [26] and Feke and colleagues [52] suggested that alterations in retinal blood flow can distinguish mild cognitive impairment and AD. Furthermore, a study by Hadoux and colleagues demonstrated significance differences in the retinal reflectance spectra when comparing PET-specific Aβ burden in mild cognitively impaired individuals with age-matched PET-negative control individuals [84]. The authors show a direct correlation between retinal imaging scores and cerebral Aβ plaque burden [84].

In this study, we used 5×FAD mice brain and retinal tissues for pathological assessment and immune-detection of age-dependent Aβo accumulation. H & E staining revealed vacuolations, neuronal loss, and presence of eosinophilic aggregates in the neocortex and hippocampus of the brain but no obvious lesions were observed in the GCL and INL of the retina. We then used Congo red and ThT staining to demonstrate age-dependent accumulation of amyloid fibrils in the retina and brain of 5×FAD mice. We show that Congophilic-amyloid fibrils increased with age in the cortex and to a lesser extent in the retina. We wanted to verify whether the staining method was sensitive enough for the detection of retinal amyloid fibrils, hence we stained with ThT. This fluorescence reaction revealed staining of retinal amyloid fibrilsin the GCL and INLof 5×FAD mice. Amyloid fibrils were observed in the neocortex and the inferior layer of the hippocampus of 6-month-old 5×FAD mice. In older 5×FAD mice, amyloid fibrils were widely distributed throughout the cortex, hippocampus, brain stem, and cerebellum. Furthermore, we used lesion specific markers for immuno detection of Aβo and Aβ plaques. In young mice (6 months), we found high levels of Aβo in the hippocampus and neocortex and in retinal layers such as theGCL and INL, and to a lesser extent the IPL and ONL. Occasional Aβ plaques were also seen in the brain and retina of this age. The middle age group (12 months) displayed both Aβo and Aβ plaques in the brain. Retinal Aβo and to lesser extent Aβ plaques were observed in this age group, indicating that the retinal microenvironment is less efficient in sustaining plaque build-up. Finally, older 5×FAD mice (17 months) displayed widespread and extensive plaque burden in both brain and retina but only traces of Aβo. Taken together, these results strongly support the Aβo conversion to plaque paradigm in the brain. Studies by Kawarabayashiand colleagues [85] using the Tg2576 AD mouse model showed that full-length unmodified Aβ was present in the brain of young littermates which then turned into soluble Aβo at 6–10 months of age, followed by insoluble forms of Aβ which increased exponentially and converted into diffuse plaques from 12 to 23 months. Similar findings were reported for theAβPP^{sw}-tau^{vlw} mouse model which displayed an age-dependent exponential increase of Aβo deposition followed by plaque build-up [86].

We extend previous experimental studies to show that Aβo strongly co-localizes with Aβ plaques in both brain and retina of 5×FAD mice. A similar pattern of age-related changes in Aβo and Aβ plaques was evident between the brain and retina of 5×FAD mice. Specifically, both show an initial accumulation of the toxic soluble Aβo entities that are converted into Aβ plaques with age.

In the 6-month-old 5×FAD mice, Aβo localized predominantly to the retinal inner and middle nuclear layers. This is an important finding as it providesa rationale for the development of imaging approaches for detecting AD manifestation in the retina. Liu and colleagues have shown that the majority of Aβ plaques were present in the GCL and IPL with some plaques found in the ONL, photoreceptor outer segment, and optic nerve in 14-month-old Tg2576 mice [87]. That ours and other preclinical studies demonstratea propensity for Aβo and Aβ plaques to localize to the inner retina is consistent with clinical observations of GCL and nerve fiber layer thinning and optic nerve degeneration in AD patients [88].

Koronyo-Hamaoui and colleagues [89] confirmed the presence of retinal Aβ plaques by systemic administration of curcumin in AβPP (SWE)/PS1 (ΔE9) mice. They confirmed presence of curcumin-positive retinal Aβ plaques in the retinal nerve fiber layer, GCL, IPL and OPL, and INL of the retina. The authors showed that plaques were detected as early as at 2.5 months of age which indicate that Aβ plaques

in the retina precede brain plaques build-up. In our study, we detected both Aβo and Aβ plaques in the retinal layers of 6-month-old 5×FAD mice. Specifically, we found that Aβo was similarin the retinal layers when compared to levels in the brain of young mice. This suggest that detection of Aβo in the retina may be a sensitive marker for early diagnosis of AD. More work is required to understand the molecular 'behavior' of both Aβo and Aβ plaques in the retina.

We confirmed that Aβo was found in neurons as evident by co-staining with NeuN [90, 91]. It was previously reported that Aβ build-up is initiated in the intracellular compartments (reviewed by Bayer and colleagues [92]). This is consistent with other reports that $A\beta_{42}$ accumulates intraneuronally before being converted into extracellular plaques in human AD [90, 93, 94]. Our findings clearly show that Aβo localized to neurons in the hippocampus, neocortex and in various retinal layers, especially in the ONL, INL and GCL in 5×FAD mice across all ages. Aβ has been found in four intraneuronal compartments associated with the lysosomal system such as rab5-positive endosomes [66], autophagic vacuoles [95], lysosomes [96, 97], and multivesicular bodies [98]. Inhibition of Aβ secretion can lead to accumulation of intraneuronal Aβ in the lysosomal compartment and destabilizes its membrane and also deposits in the cytosolic compartment in the early AD pathogenesis [99]. In agreement, we show that Aβo co-localizes to late endosomes in retinal cells, indicating that disturbance of the endocytic pathway leads to its accumulation [100, 101].

Conclusion

Our study demonstrated an age-dependent inversely proportional accumulation of Aβo versus Aβ plaques in the retina of a transgenic AD animal model. The presence of these toxic Aβ soluble oligomers was detected as early as 6 months of age in this animal model, probably mimicking prodromal human AD pathogenesis. More work is needed in earlier age groups perhaps using a less 'aggressive' animal model in order to prove that the toxic assemblies can be detected in the retina before identification of cognitive deficiencies. Studies are currently underway to establish this before the useof fluorescence confocal scanning laser ophthalmoscopy for the non-invasive detection of retinal Aβo preceding their accumulation in the brain.

ACKNOWLEDGMENTS

We wish to thank Dr. Hong Yu at the West mead Institute for Medical Research, Sydney, Australia for help with image acquisition using the Olympus VS 120.

The Laboratory of Dr. MT received Institutional Start Up support and a Post-Graduate Scholarship for UH.

Authors' disclosures available online (https://www.j-alz.com/manuscript-disclosures/19-1346r2).

AVAILABILITY OF DATA AND MATERIALS

The datasets generated during this study are available from the corresponding author on request.

SUPPLEMENTARY MATERIAL

The supplementary material is available in the electronic version of this article: https://dx.doi.org/10.3233/JAD-191346.

REFERENCES

[1] Beyreuther K, Masters CL (1991) Amyloid precursor protein (APP) and beta A4 amyloid in the etiology of Alzheimer's disease: Precursor-product relationships in the derangement of neuronal function. *Brain Pathol* **1**, 241-251.

[2] Mott RT, Hulette CM (2005) Neuropathology of Alzheimer's disease. *Neuroimaging Clin N Am* **15**, 755-765, ix.

[3] Perl DP (2010) Neuropathology of Alzheimer's disease. *Mt Sinai J Med* **77**, 32-42.

[4] Selkoe DJ, Hardy J (2016) The amyloid hypothesis of Alzheimer's disease at 25 years. *EMBO Mol Med* **8**, 595-608.

[5] Clark CM, Karlawish JH (2003) Alzheimer disease: Current concepts and emerging diagnostic and therapeutic strategies. *Ann Intern Med* **138**, 400-410.

[6] Serrano-Pozo A, Frosch MP, Masliah E, Hyman BT (2011) Neuropathological alterations in Alzheimer disease. *Cold Spring Harb Perspect Med* **1**, a006189.

[7] Cai XD, Golde TE, Younkin SG (1993) Release of excess amyloid beta protein from a mutant amyloid beta protein precursor. *Science* **259**, 514-516.

[8] Kang J, Lemaire HG, Unterbeck A, Salbaum JM, Masters CL, Grzeschik KH, Multhaup G, Beyreuther K, Müller-Hill B (1987) The precursor of Alzheimer's disease amyloid A4 protein resembles a cell-surface receptor. *Nature* **325**, 733-736.

[9] Suzuki N, Cheung TT, Cai XD, Odaka A, Otvos L, Jr., Eckman C, Golde TE, Younkin SG (1994) An increased percentage of long amyloid beta protein secreted by familial amyloid beta protein precursor (beta APP717) mutants. *Science* **264**, 1336-1340.

[10] Chow VW, Mattson MP, Wong PC, Gleichmann M (2010) An overview of APP processing enzymes and products. *Neuromolecular Med* **12**, 1-12.

[11] Sengupta U, Nilson AN, Kayed R (2016) The role of Amyloid-β oligomers in toxicity, propagation, and immunotherapy. *EBioMedicine* **6**, 42-49.

[12] Alafuzoff I, Arzberger T, Al-Sarraj S, Bodi I, Bogdanovic N, Braak H, Bugiani O, Del-Tredici K, Ferrer I, Gelpi E, Giaccone G, Graeber MB, Ince P, Kamphorst W, King A, Korkolopoulou P, Kovács GG, Larionov S, Meyronet D, Monoranu C, Parchi P, Patsouris E, Roggendorf W, Seilhean D, Tagliavini F, Stadelmann C, Streichenberger N, Thal DR, Wharton SB, Kretzschmar H (2008) Staging of neurofibrillary pathology in Alzheimer's disease: A study of the BrainNet Europe Consortium. *Brain Pathol* **18**, 484-496.

[13] Murphy MP, LeVine H, 3rd (2010) Alzheimer's disease and the amyloid-beta peptide. *J Alzheimers Dis* **19**, 311-323.

[14] Broersen K, Rousseau F, Schymkowitz J (2010) The culprit behind amyloid beta peptide related neurotoxicity in Alzheimer's disease: Oligomer size or conformation? *Alzheimers Res Ther* **2**, 12.

[15] Goure WF, Krafft GA, Jerecic J, Hefti F (2014) Targeting the proper amyloid-beta neuronal toxins: A path forward for Alzheimer's disease immunotherapeutics. *Alzheimers Res Ther* **6**, 42.

[16] Glabe CG (2008) Structural classification of toxic amyloid oligomers. *J Biol Chem* **283**, 29639-29643.

[17] Mroczko B, Groblewska M, Litman-Zawadzka A, Kornhuber J, Lewczuk P (2018) Amyloid β oligomers (AβOs) in Alzheimer's disease. *J Neural Transm (Vienna)* **125**, 177-191.

[18] Benilova I, Karran E, De Strooper B (2012) The toxic Aβ oligomer and Alzheimer's disease: An emperor in need of clothes. *Nat Neurosci* **15**, 349-357.

[19] Haass C, Selkoe DJ (2007) Soluble protein oligomers in neurodegeneration: Lessons from the Alzheimer's amyloid beta-peptide. *Nat Rev Mol Cell Biol* **8**, 101-112.

[20] Kayed R, Head E, Thompson JL, McIntire TM, Milton SC, Cotman CW, Glabe CG (2003) Common structure of soluble amyloid oligomers implies common mechanism of pathogenesis. *Science* **300**, 486-489.

[21] Zhao LN, Long H, Mu Y, Chew LY (2012) The toxicity of amyloid β oligomers. *Int J Mol Sci* **13**, 7303-7327.

[22] Frackowiak J, Zoltowska A, Wisniewski HM (1994) Non-fibrillar beta-amyloid protein is associated with smooth muscle cells of vessel walls in Alzheimer disease. *J Neuropathol Exp Neurol* **53**, 637-645.

[23] Viola KL, Klein WL (2015) Amyloid β oligomers in Alzheimer's disease pathogenesis, treatment, and diagnosis. *Acta Neuropathol* **129**, 183-206.

[24] Katz B, Rimmer S (1989) Ophthalmologic manifestations of Alzheimer's disease. *Surv Ophthalmol* **34**, 31-43.

[25] Sadun AA, Borchert M, DeVita E, Hinton DR, Bassi CJ (1987) Assessment of visual impairment in patients with Alzheimer's disease. *Am J Ophthalmol* **104**, 113-120.

[26] Berisha F, Feke GT, Trempe CL, McMeel JW, Schepens CL (2007) Retinal abnormalities in early Alzheimer's disease. *Invest Ophthalmol Vis Sci* **48**, 2285-2289.

[27] Frost S, Kanagasingam Y, Sohrabi H, Vignarajan J, Bourgeat P, Salvado O, Villemagne V, Rowe CC, Macaulay SL, Szoeke C, Ellis KA, Ames D, Masters CL, Rainey-Smith S, Martins RN, Group AR (2013) Retinal vascular biomarkers for early detection and monitoring of Alzheimer's disease. *Transl Psychiatry* **3**, e233.

[28] Paquet C, Boissonnot M, Roger F, Dighiero P, Gil R, Hugon J (2007) Abnormal retinal thickness in patients with mild cognitive impairment and Alzheimer's disease. *Neurosci Lett* **420**, 97-99.

[29] Fotiou DF, Brozou CG, Haidich AB, Tsiptsios D, Nakou M, Kabitsi A, Giantselidis C, Fotiou F (2007) Pupil reaction to light in Alzheimer's disease: Evaluation of pupil size changes and mobility. *Aging Clin Exp Res* **19**, 364-371.

[30] Frost S, Kanagasingam Y, Sohrabi H, Bourgeat P, Villemagne V, Rowe CC, Macaulay SL, Szoeke C, Ellis KA, Ames D, Masters CL, Rainey-Smith S, Martins RN (2013) Pupil response biomarkers for early detection and monitoring of Alzheimer's disease. *Curr Alzheimer Res* **10**, 931-939.

[31] Lim JK, Li QX, He Z, Vingrys AJ, Wong VH, Currier N, Mullen J, Bui BV, Nguyen CT (2016) The eye as a biomarker for Alzheimer's disease. *Front Neurosci* **10**, 536.

[32] Nguyen CTO, Hui F, Charng J, Velaedan S, van Koeverden AK, Lim JKH, He Z, Wong VHY, Vingrys AJ, Bui BV, Ivarsson M (2017) Retinal biomarkers provide "insight" into cortical pharmacology and disease. *Pharmacol Ther* **175**, 151-177.

[33] Cronin-Golomb A, Corkin S, Rizzo JF, Cohen J, Growdon JH, Banks KS (1991) Visual dysfunction in Alzheimer's disease: Relation to normal aging. *Ann Neurol* **29**, 41-52.

[34] Cronin-Golomb A, Sugiura R, Corkin S, Growdon JH (1993) Incomplete achromatopsia in Alzheimer's disease. *Neurobiol Aging* **14**, 471-477.

[35] Armstrong RA, Winsper SJ, Blair JA (1996) Aluminium and Alzheimer's disease: Review of possible pathogenic mechanisms. *Dementia* **7**, 1-9.

[36] Trick GL, Trick LR, Morris P, Wolf M (1995) Visual field loss in senile dementia of the Alzheimer's type. *Neurology* **45**, 68-74.

[37] Valenti DA (2013) Alzheimer's disease: Screening biomarkers using frequency doubling technology visual field. *ISRN Neurol* **2013**, 989583.

[38] Rizzo M, Anderson SW, Dawson J, Nawrot M (2000) Vision and cognition in Alzheimer's disease. *Neuropsychologia* **38**, 1157-1169.

[39] Danesh-Meyer HV, Birch H, Ku JY, Carroll S, Gamble G (2006) Reduction of optic nerve fibers in patients with Alzheimer disease identified by laser imaging. *Neurology* **67**, 1852-1854.

[40] Blanks JC, Torigoe Y, Hinton DR, Blanks RH (1996) Retinal pathology in Alzheimer's disease. I. Ganglion cell loss in foveal/parafoveal retina. *Neurobiol Aging* **17**, 377-384.

[41] Sadun AA, Bassi CJ (1990) Optic nerve damage in Alzheimer's disease. *Ophthalmology* **97**, 9-17.

[42] Blanks JC, Hinton DR, Sadun AA, Miller CA (1989) Retinal ganglion cell degeneration in Alzheimer's disease. *Brain Res* **501**, 364-372.

[43] Blanks JC, Schmidt SY, Torigoe Y, Porrello KV, Hinton DR, Blanks RH (1996) Retinal pathology in Alzheimer's disease. II. Regional neuron loss and glial changes in GCL. *Neurobiol Aging* **17**, 385-395.

[44] Colligris P, Perez de Lara MJ, Colligris B, Pintor J (2018) Ocular manifestations of Alzheimer's and other neurodegenerative diseases: The prospect of the eye as a tool for the early diagnosis of Alzheimer's disease. *J Ophthalmol* **2018**, 8538573.

[45] Dutescu RM, Li QX, Crowston J, Masters CL, Baird PN, Culvenor JG (2009) Amyloid precursor protein processing and retinal pathology in mouse models of Alzheimer's disease. *Graefes Arch Clin Exp Ophthalmol* **247**, 1213-1221.

[46] Hinton DR, Sadun AA, Blanks JC, Miller CA (1986) Optic-nerve degeneration in Alzheimer's disease. *N Engl J Med* **315**, 485-487.

[47] Koronyo Y, Biggs D, Barron E, Boyer DS, Pearlman JA, Au WJ, Kile SJ, Blanco A, Fuchs DT, Ashfaq A, Frautschy S, Cole GM, Miller CA, Hinton DR, Verdooner SR, Black KL, Koronyo-Hamaoui M (2017) Retinal amyloid pathology and proof-of-concept imaging trial in Alzheimer's disease. *JCI Insight* **2**, e93621.

[48] La Morgia C, Ross-Cisneros FN, Koronyo Y, Hannibal J, Gallassi R, Cantalupo G, Sambati L, Pan BX, Tozer KR, Barboni P, Provini F, Avanzini P, Carbonelli M, Pelosi A, Chui H, Liguori R, Baruzzi A, Koronyo-Hamaoui M, Sadun AA, Carelli V (2016) Melanopsin retinal ganglion cell loss in Alzheimer disease. *Ann Neurol* **79**, 90-109.

[49] Lu Y, Li Z, Zhang X, Ming B, Jia J, Wang R, Ma D (2010) Retinal nerve fiber layer structure abnormalities in early Alzheimer's disease: Evidence in optical coherence tomography. *Neurosci Lett* **480**, 69-72.

[50] Iseri PK, Altinaş O, Tokay T, Yüksel N (2006) Relationship between cognitive impairment and retinal morphological and visual functional abnormalities in Alzheimer disease. *J Neuroophthalmol* **26**, 18-24.

[51] O'Bryhim BE, Apte RS, Kung N, Coble D, Van Stavern GP (2018) Association of preclinical Alzheimer disease with optical coherence tomographic angiography findings. *JAMA Ophthalmol* **136**, 1242-1248.

[52] Feke GT, Hyman BT, Stern RA, Pasquale LR (2015) Retinal blood flow in mild cognitive impairment and Alzheimer's disease. *Alzheimers Dement (Amst)* **1**, 144-151.

[53] Ratnayaka JA, Serpell LC, Lotery AJ (2015) Dementia of the eye: The role of amyloid beta in retinal degeneration. *Eye (Lond)* **29**, 1013-1026.

[54] Williams MA, McGowan AJ, Cardwell CR, Cheung CY, Craig D, Passmore P, Silvestri G, Maxwell AP, McKay GJ (2015) Retinal microvascular network attenuation in Alzheimer's disease. *Alzheimers Dement (Amst)* **1**, 229-235.

[55] Oakley H, Cole SL, Logan S, Maus E, Shao P, Craft J, Guillozet-Bongaarts A, Ohno M, Disterhoft J, Van Eldik L, Berry R, Vassar R (2006) Intraneuronal beta-amyloid aggregates, neurodegeneration, and neuron loss in transgenic mice with five familial Alzheimer's disease mutations: Potential factors in amyloid plaque formation. *J Neurosci* **26**, 10129-10140.

[56] Anstee DJ, Gardner B, Spring FA, Holmes CH, Simpson KL, Parsons SF, Mallinson G, Yousaf SM, Judson PA (1991) New monoclonal antibodies in CD44 and CD58: Their use to quantify CD44 and CD58 on normal human erythrocytes and to compare the distribution of CD44 and CD58 in human tissues. *Immunology* **74**, 197-205.

[57] Avent ND, Ridgwell K, Mawby WJ, Tanner MJ, Anstee DJ, Kumpel B (1988) Protein-sequence studies on Rh-related polypeptides suggest the presence of at least two groups of proteins which associate in the human red-cell membrane. *Biochem J* **256**, 1043-1046.

[58] Hardy J, Allsop D (1991) Amyloid deposition as the central event in the aetiology of Alzheimer's disease. *Trends Pharmacol Sci* **12**, 383-388.

[59] Teboul O, Feki A, Dubois A, Bozon B, Faure A, Hantraye P, Dhenain M, Delatour B, Delzescaux T (2007) A standardized method to automatically segment amyloid plaques in Congo Red stained sections from Alzheimer transgenic mice. *Conf Proc IEEE Eng Med Biol Soc* **2007**, 5593-5596.

[60] Hardy J, Selkoe DJ (2002) The amyloid hypothesis of Alzheimer's disease: Progress and problems on the road to therapeutics. *Science* **297**, 353-356.

[61] Laske C, Sohrabi HR, Frost SM, López-de-Ipiña K, Garrard P, Buscema M, Dauwels J, Soekadar SR, Mueller S, Linnemann C, Bridenbaugh SA, Kanagasingam Y, Martins RN, O'Bryant SE (2015) Innovative diagnostic tools for early detection of Alzheimer's disease. *Alzheimers Dement* **11**, 561-578.

[62] Schindler SE, Bollinger JG, Ovod V, Mawuenyega KG, Li Y, Gordon BA, Holtzman DM, Morris JC, Benzinger TLS, Xiong C, Fagan AM, Bateman RJ (2019) High-precision plasma β-amyloid 42/40 predicts current and future brain amyloidosis. *Neurology* **93**, e1647-e1659.

[63] Wang MJ, Yi S, Han JY, Park SY, Jang JW, Chun IK, Kim SE, Lee BS, Kim GJ, Yu JS, Lim K, Kang SM, Park YH, Youn YC, An SSA, Kim S (2017) Oligomeric forms of amyloid-β protein in plasma as a potential blood-based biomarker for Alzheimer's disease. *Alzheimers Res Ther* **9**, 98.

[64] Criscuolo C, Cerri E, Fabiani C, Capsoni S, Cattaneo A, Domenici L (2018) The retina as a window to early dysfunctions of Alzheimer's disease following studies with a 5xFAD mouse model. *Neurobiol Aging* **67**, 181-188.

[65] Adamec E, Mohan PS, Cataldo AM, Vonsattel JP, Nixon RA (2000) Up-regulation of the lysosomal system in experimental models of neuronal injury: Implications for Alzheimer's disease. *Neuroscience* **100**, 663-675.

[66] Cataldo AM, Petanceska S, Terio NB, Peterhoff CM, Durham R, Mercken M, Mehta PD, Buxbaum J, Haroutunian V, Nixon RA (2004) Abeta localization in abnormal endosomes: Association with earliest Abeta elevations in AD and Down syndrome. *Neurobiol Aging* **25**, 1263-1272.

[67] Pasternak SH, Callahan JW, Mahuran DJ (2004) The role of the endosomal/lysosomal system in amyloid-beta production and the pathophysiology of Alzheimer's disease: Reexamining the spatial paradox from a lysosomal perspective. *J Alzheimers Dis* **6**, 53-65.

[68] Wolfe DM, Lee JH, Kumar A, Lee S, Orenstein SJ, Nixon RA (2013) Autophagy failure in Alzheimer's disease and the role of defective lysosomal acidification. *Eur J Neurosci* **37**, 1949-1961.

[69] El-Agnaf OM, Salem SA, Paleologou KE, Curran MD, Gibson MJ, Court JA, Schlossmacher MG, Allsop D (2006) Detection of oligomeric forms of alpha-synuclein protein in human plasma as a potential biomarker for Parkinson's disease. *FASEB J* **20**, 419-425.

[70] McKhann GM, Knopman DS, Chertkow H, Hyman BT, Jack CR, Jr., Kawas CH, Klunk WE, Koroshetz WJ, Manly JJ, Mayeux R, Mohs RC, Morris JC, Rossor MN, Scheltens P, Carrillo MC, Thies B, Weintraub S, Phelps CH (2011) The diagnosis of dementia due to Alzheimer's disease: Recommendations from the National Institute on Aging-Alzheimer's Association workgroups on diagnostic guidelines for Alzheimer's disease. *Alzheimers Dement* **7**, 263-269.

[71] El-Agnaf OM, Walsh DM, Allsop D (2003) Soluble oligomers for the diagnosis of neurodegenerative diseases. *Lancet Neurol* **2**, 461-462.

[72] Doecke JD, Laws SM, Faux NG, Wilson W, Burnham SC, Lam CP, Mondal A, Bedo J, Bush AI, Brown B, De Ruyck K, Ellis KA, Fowler C, Gupta VB, Head R, Macaulay SL, Pertile K, Rowe CC, Rembach A, Rodrigues M, Rumble R, Szoeke C, Taddei K, Taddei T, Trounson B, Ames D, Masters CL, Martins RN (2012) Blood-based protein biomarkers for diagnosis of Alzheimer disease. *Arch Neurol* **69**, 1318-1325.

[73] Snyder HM, Carrillo MC, Grodstein F, Henriksen K, Jeromin A, Lovestone S, Mielke MM, O'Bryant S, Sarasa M, Sjøgren M, Soares H, Teeling J, Trushina E, Ward M, West T, Bain LJ, Shineman DW, Weiner M, Fillit HM (2014) Developing novel blood-based biomarkers for Alzheimer's disease. *Alzheimers Dement* **10**, 109-114.

[74] Gong Y, Chang L, Viola KL, Lacor PN, Lambert MP, Finch CE, Krafft GA, Klein WL (2003) Alzheimer's disease-affected brain: Presence of oligomeric A beta ligands (ADDLs) suggests a molecular basis for reversible memory loss. *Proc Natl Acad Sci U S A* **100**, 10417-10422.

[75] Larson ME, Lesné SE (2012) Soluble Aβ oligomer production and toxicity. *J Neurochem* **120 Suppl 1**, 125-139.

[76] Lesné SE, Sherman MA, Grant M, Kuskowski M, Schneider JA, Bennett DA, Ashe KH (2013) Brain amyloid-β oligomers in ageing and Alzheimer's disease. *Brain* **136**, 1383-1398.

[77] Sakono M, Zako T (2010) Amyloid oligomers: Formation and toxicity of Abeta oligomers. *FEBS J* **277**, 1348-1358.

[78] Santos AN, Simm A, Holthoff V, Boehm G (2008) A method for the detection of amyloid-beta1-40, amyloid-beta1-42 and amyloid-beta oligomers in blood using magnetic beads in combination with flow cytometry and its application in the diagnostics of Alzheimer's disease. *J Alzheimers Dis* **14**, 127-131.

[79] Xia W, Yang T, Shankar G, Smith IM, Shen Y, Walsh DM, Selkoe DJ (2009) A specific enzyme-linked immunosorbent assay for measuring beta-amyloid protein oligomers in human plasma and brain tissue of patients with Alzheimer disease. *Arch Neurol* **66**, 190-199.

[80] Zhou L, Chan KH, Chu LW, Kwan JS, Song YQ, Chen LH, Ho PW, Cheng OY, Ho JW, Lam KS (2012) Plasma amyloid-β oligomers level is a biomarker for Alzheimer's disease diagnosis. *Biochem Biophys Res Commun* **423**, 697-702.

[81] Nakamura A, Kaneko N, Villemagne VL, Kato T, Doecke J, Doré V, Fowler C, Li QX, Martins R, Rowe C, Tomita T, Matsuzaki K, Ishii K, Ishii K, Arahata Y, Iwamoto S, Ito K, Tanaka K, Masters CL, Yanagisawa K (2018) High performance plasma amyloid-β biomarkers for Alzheimer's disease. *Nature* **554**, 249-254.

[82] Zachary JF, McGavin MD (2016) *Pathologic Basis of Veterinary Disease Expert Consult-E-BOOK*, Elsevier Health Sciences.

[83] Armstrong RA (2009) Alzheimer's disease and the eye. *J Optom* **2**, 103-111.

[84] Hadoux X, Hui F, Lim JKH, Masters CL, Pébay A, Chevalier S, Ha J, Loi S, Fowler CJ, Rowe C, Villemagne VL, Taylor EN, Fluke C, Soucy JP, Lesage F, Sylvestre JP, Rosa-Neto P, Mathotaarachchi S, Gauthier S, Nasreddine ZS, Arbour JD, Rhéaume MA, Beaulieu S, Dirani M, Nguyen CTO, Bui BV, Williamson R, Crowston JG, van Wijngaarden P (2019) Non-invasive in vivo hyperspectral imaging of the retina for potential biomarker use in Alzheimer's disease. *Nat Commun* **10**, 4227.

[85] Kawarabayashi T, Younkin LH, Saido TC, Shoji M, Ashe KH, Younkin SG (2001) Age-dependent changes in brain, CSF, and plasma amyloid (beta) protein in the Tg2576 transgenic mouse model of Alzheimer's disease. *J Neurosci* **21**, 372-381.

[86] DaRocha-Souto B, Scotton TC, Coma M, Serrano-Pozo A, Hashimoto T, Serenó L, Rodríguez M, Sánchez B, Hyman BT, Gómez-Isla T (2011) Brain oligomeric β-amyloid but not total amyloid plaque burden correlates with neuronal loss and astrocyte inflammatory response in amyloid precursor protein/tau transgenic mice. *J Neuropathol Exp Neurol* **70**, 360-376.

[87] Liu B, Rasool S, Yang Z, Glabe CG, Schreiber SS, Ge J, Tan Z (2009) Amyloid-peptide vaccinations reduce {beta}-amyloid plaques but exacerbate vascular deposition and inflammation in the retina of Alzheimer's transgenic mice. *Am J Pathol* **175**, 2099-2110.

[88] Morin PJ, Abraham CR, Amaratunga A, Johnson RJ, Huber G, Sandell JH, Fine RE (1993) Amyloid precursor protein is synthesized by retinal ganglion cells, rapidly transported to the optic nerve plasma membrane and nerve terminals, and metabolized. *J Neurochem* **61**, 464-473.

[89] Koronyo-Hamaoui M, Koronyo Y, Ljubimov AV, Miller CA, Ko MK, Black KL, Schwartz M, Farkas DL (2011) Identification of amyloid plaques in retinas from Alzheimer's patients and noninvasive in vivo optical imaging of retinal plaques in a mouse model. *Neuroimage* **54 Suppl 1**, S204-217.

[90] Gouras GK, Tsai J, Naslund J, Vincent B, Edgar M, Checler F, Greenfield JP, Haroutunian V, Buxbaum JD, Xu H, Greengard P, Relkin NR (2000) Intraneuronal Abeta42 accumulation in human brain. *Am J Pathol* **156**, 15-20.

[91] Umeda T, Tomiyama T, Sakama N, Tanaka S, Lambert MP, Klein WL, Mori H (2011) Intraneuronal amyloid β oligomers cause cell death via endoplasmic reticulum stress, endosomal/lysosomal leakage, and mitochondrial dysfunction in vivo. *J Neurosci Res* **89**, 1031-1042.

[92] Bayer TA, Wirths O, Majtényi K, Hartmann T, Multhaup G, Beyreuther K, Czech C (2001) Key factors in Alzheimer's disease: Beta-amyloid precursor protein processing, metabolism and intraneuronal transport. *Brain Pathol* **11**, 1-11.

[93] Iwatsubo T, Odaka A, Suzuki N, Mizusawa H, Nukina N, Ihara Y (1994) Visualization of A beta 42(43) and A beta 40 in senile plaques with end-specific A beta monoclonals: Evidence that an initially deposited species is A beta 42(43). *Neuron* **13**, 45-53.

[94] Wirths O, Multhaup G, Czech C, Blanchard V, Moussaoui S, Tremp G, Pradier L, Beyreuther K, Bayer TA (2001) Intraneuronal Abeta accumulation precedes plaque formation in beta-amyloid precursor protein and presenilin-1 double-transgenic mice. *Neurosci Lett* **306**, 116-120.

[95] Yu WH, Cuervo AM, Kumar A, Peterhoff CM, Schmidt SD, Lee JH, Mohan PS, Mercken M, Farmery MR, Tjernberg LO, Jiang Y, Duff K, Uchiyama Y, Näslund J, Mathews PM, Cataldo AM, Nixon RA (2005) Macroautophagy–a novel Beta-amyloid peptide-generating pathway activated in Alzheimer's disease. *J Cell Biol* **171**, 87-98.

[96] Langui D, Girardot N, El Hachimi KH, Allinquant B, Blanchard V, Pradier L, Duyckaerts C (2004) Subcellular topography of neuronal Abeta peptide in APPxPS1 transgenic mice. *Am J Pathol* **165**, 1465-1477.

[97] Zheng L, Kågedal K, Dehvari N, Benedikz E, Cowburn R, Marcusson J, Terman A (2009) Oxidative stress induces macroautophagy of amyloid beta-protein and ensuing apoptosis. *Free Radic Biol Med* **46**, 422-429.

[98] Takahashi RH, Milner TA, Li F, Nam EE, Edgar MA, Yamaguchi H, Beal MF, Xu H, Greengard P, Gouras GK (2002) Intraneuronal Alzheimer abeta42 accumulates in multivesicular bodies and is associated with synaptic pathology. *Am J Pathol* **161**, 1869-1879.

[99] Yang AJ, Chandswangbhuvana D, Margol L, Glabe CG (1998) Loss of endosomal/lysosomal membrane impermeability is an early event in amyloid Abeta1-42 pathogenesis. *J Neurosci Res* **52**, 691-698.

[100] Yu C, Nwabuisi-Heath E, Laxton K, Ladu MJ (2010) Endocytic pathways mediating oligomeric Abeta42 neurotoxicity. *Mol Neurodegener* **5**, 19.

[101] Zheng L, Cedazo-Minguez A, Hallbeck M, Jerhammar F, Marcusson J, Terman A (2012) Intracellular distribution of amyloid beta peptide and its relationship to the lysosomal system. *Transl Neurodegener* **1**, 19.